Green Chemistry

Accepted Manuscript

ROYAL SOCIETY OF CHEMISTRY

rsc.li/green-chem

View Article Online
DOI: 10.1039/C7GC02764H

Journal Name

ARTICLE

Solvent- and Base-Free Synthesis of Wax Esters from Fatty Acid Methyl Esters by Consecutive One-Pot, Two-Step Catalysis.

Received 00th January 20xx,
Accepted 00th January 20xx

DOI: 10.1039/x0xx00000x

www.rsc.org/

D. H. Nguyen,[a] G. Raffa,[a] Y. Morin,[a] S. Desset,[a] F. Capet,[a] V. Nardello-Rataj,[a] F. Dumeignil*[a], R. M. Gauvin*[a]

Abstract: One-pot, two-step synthesis of wax esters was successfully conducted by consecutive homogenous ruthenium-catalysed hydrogenation-dehydrogenation reactions of fatty acid methyl esters, in the absence of solvent and of base additive. Under optimized conditions, excellent conversion and selectivity were reached. Furthermore, physicochemical investigations revealed that the resulting compounds display properties similar to benchmark commercial products extracted from natural sources of lesser availability compared to the herein considered bioresources, making this chemical route very promising regarding further potential industrial implementation.

Introduction

Wax esters are a class of commodity materials widely used as cosmetics, lubricating agents, plasticizers and surface coatings, *inter alia*.[1] This owes to their specific characteristics, such as non-toxicity, biodegradability and physicochemical properties ideally suited for the above-mentioned industrial applications. These compounds formally result from condensation of long-chain carboxylic acids and alcohols, occasionally featuring unsaturations. Chain length and degree of branching and of unsaturation affect their melting temperature, oxidation stability as well as thermal stability, for instance.

The vast majority of wax esters are bio-sourced, either from animal or vegetal origin. Among these, sperm whale oil, mostly composed of cetyl palmitate (C_{16}-C_{16}, Figure 1), was widely used as oil lamp fuel, lubricant or ingredient for cosmetics. Due to whale hunt banning, this material ceased to be available, and alternative products were sought. Jojoba oil was soon acknowledged as a most suitable substitute.[2] This oil, extracted from the nut of jojoba bush, consists mostly of mono-unsaturated esters featuring in total between 34 and 50 carbon atoms.[3] Its market share is in expansion, mainly in the cosmetics sector. However, several drawbacks, such as farming in semi-arid regions or delay until seed availability (more than 5 years after planting), limit the volume of this product on the market and have negative impact on bulk prices: Jojoba oil is available in insufficient quantities at a very high price, which limits its use to pharmaceutics and cosmetics. Thus, considering the high potential of such compounds in high value-added industrial segments such as high-performance lubricants, or as components in plasticizers and stabilizers, an efficient synthetic access is highly attractive.

To circumvent these issues, alternative bio-resources have been identified as entry points to synthetic wax esters, either using enzymatic or chemical routes. Thus, among the many bio-catalytic methods reported so far, lipase-catalysed synthesis of wax esters from esterification of fatty acids and alcohols has drawn much attention, as these environmentally-benign processes are usually performed with high selectivity under mild conditions (atmospheric pressure, moderate pH and temperature).[4] However, these suffer from low productivity and challenging scale-up, requiring very specific reactor design to ensure commercially competitive reaction rate and catalyst stability.[5]

On the other hand, the classical chemical/synthetic approach is typically a multi-step, waste-generating process: fatty alcohols have first to be generated from (stoichiometric) reduction of carboxylic acid derivatives, prior to esterification with long-chain acids or acyl chlorides or transesterification with fatty esters. For instance, industrial processes used to prepare wax esters make use of tin-based catalysts at high temperature, which requires extensive downstream purification.[6] There is thus clearly a need for the implementation of novel, selective and environmentally-benign processes for the production of wax esters from readily

[a] Univ. Lille, CNRS, Centrale Lille, ENSCL, Univ. Artois, UMR 8181 - UCCS - Unité de Catalyse et Chimie du Solide, F-59000 Lille, France.
* Corresponding authors: Franck.Dumeignil@univ-lille1.fr, Regis.Gauvin@ensc-lille.fr.
Electronic Supplementary Information (ESI) available: NMR characterization of **3**, kinetic studies on the formation of **3**, ^{1}H NMR spectra of catalytic reaction solutions, physico-chemical property measurements on wax esters. See DOI: 10.1039/x0xx00000x

View Article Online
DOI: 10.1039/C7GC02764H

available bio-sourced compounds.

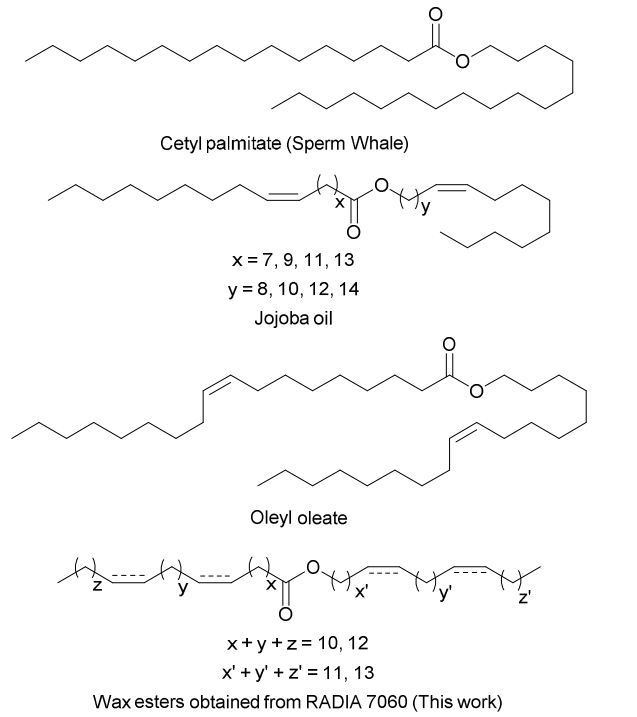

Figure 1. Relevant wax esters found in nature and considered in this work.

When discussing catalytic processes related to esters and alcohols chemistry, one must consider the breakthrough accomplished thanks to metal-ligand cooperative organometallic systems.[7] These enable highly efficient conversion of alcohols into esters through acceptorless dehydrogenative coupling, as well as the reverse reaction (ester hydrogenation).[8] Reasoning on these points, we envisioned to tackle the issue of wax esters synthesis by starting from fatty acid methyl esters (FAMEs), which are readily available from conventional crops and currently used for biodiesel large-scale applications, *inter alia*. Our strategy relies on the use of a single catalyst in a one-pot, two-step sequence: the neat methyl ester is first hydrogenated into fatty alcohol, which is then coupled into the symmetrical wax ester with release of dihydrogen (Scheme 1). We will thus show how this can be achieved with high efficiency and selectivity starting from a commercial FAME mixture, affording wax esters with physicochemical properties comparable to those of current commercial products.

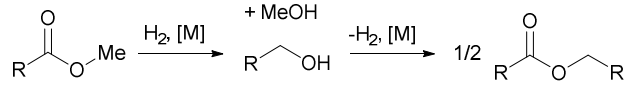

Scheme 1. Synthesis of symmetrical esters by consecutive metal-catalyzed hydrogenation-dehydrogenation reactions.

Results and discussion

Although hydrogenation of esters promoted by Ru[9], Os[10], Ir[11] and, more recently, by earth-abundant Fe,[12] Co[13] and Mn[15] complexes in the presence of a strong base has been intensively studied, very few examples were demonstrated under base-free conditions.[11b,12b,12c,15] For the sake of development of greener reduction processes, we therefore examined the hydrogenation of esters in the absence of a base, and under solvent-free conditions, namely in neat substrate. Commercially or readily available borohydride PNP-pincer ruthenium derivatives **1** and **2** were chosen as catalysts due to their activity at very low catalyst loading under comparatively mild conditions in related reactions (Figure 2).[16] Methyl heptanoate was used as benchmark substrate to optimize reaction conditions (temperature, H_2 pressure, reaction time and stirring rate). In the presence of 0.1 mol% of **1** as catalyst, under 20 bar of H_2 and with stirring rate of about 600 rpm and at 110 °C, very good conversion of methyl heptanoate (96%) was reached, with selectivity toward the desired heptan-1-ol as high as 95% after 1h (Entry 1, Table 1). The formation of the symmetric heptyl heptanoate ester was also observed (about 5% selectivity). This may be explained by the classical transesterification or/and the reverse acceptorless dehydrogenative coupling reaction (see below, though this is rather unfavoured under H_2 pressure). Performing the reaction for longer reaction times (2 h) resulted in improvement of conversion (97%) and selectivity (98%) into heptan-1-ol (Entry 2, Table 1).

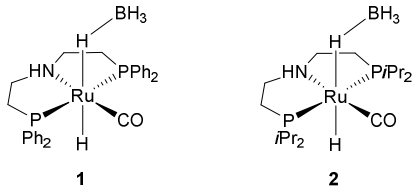

Figure 2. Precatalysts used for this study.

Influence of stirring rate was investigated next. At stirring rate of 1200 rpm, conversion of 99% is achieved within 1 h, with selectivity toward the alcohol up to 99% (Entry 3, Table 1). Lowering reaction temperature to 90 °C has only marginal impact on catalytic performances, affording conversion and selectivity values of 97 and 98 %, respectively (Entry 4, Table 1). This indicates that over the considered temperature range, this parameter exerts only minor influence on catalytic efficiency. On the opposite, lowering hydrogen pressure from 20 to 10 bar leads to both lower conversion and selectivity (Entry 5 vs. 3, Table 1). As observed above, decreasing further the temperature from 110 to 90 °C does not significantly impact on the catalytic activity (Entry 6 vs. 5, Table 1). Finally, scale-up of the hydrogenation reaction was carried out with 150 mL of methyl heptanoate and in presence of 0.2 mol% of **1** and at 1200 rpm (Entry 7, Table 1). Very good conversion of 91% was obtained with 94% selectivity toward heptan-1-ol.

View Article Online
DOI: 10.1039/C7GC02764H

Table 1. Ru-catalysed hydrogenation of methyl heptanoate.[a]

Entry	[Ru] (mol %)	$P(H_2)$ (Bar)	T (°C)	t(h)	rpm	Conv. (%)[b]	Select. (%)[c]
1	**1** (0.1)	20	110	1	600	96	95
2	**1** (0.1)	20	110	2	600	97	98
3	**1** (0.1)	20	110	1	1200	99	99
4	**1** (0.1)	20	90	2	1200	97	98
5	**1** (0.1)	10	110	2	1200	91	90
6	**1** (0.1)	10	90	2	1200	92	93
7[d]	**1** (0.2)	20	110	2	1200	91	94

[a]: V(methyl heptanoate) = 7 mL (42.23 mmol); [b] Conversion of methyl heptanoate, determined by ^{1}H NMR; [c] Selectivity towards heptan-1-ol, determined by ^{1}H NMR ; [d] V(methyl heptanoate) = 150 mL (904.93 mmol).

We next studied the hydrogenation of oleyl oleate (99%, Aldrich) that was purified prior use (See below discussions on the impact of substrate purification on catalytic activity). At 0.1 mol% of **1**, 99% of oleyl oleate was converted into the oleyl alcohol with 98% selectivity (Entry 1, Table 2). Oleic alcohol is the major product along with a small amount of oleyl oleate, as already observed in the case of methyl heptanoate. Moreover, no products generated from hydrogenation of double C=C bond were observed, indicating that hydrogenation is chemo-selective towards the C=O bond reduction. With lower catalyst loading, lower conversion was achieved, namely 64 and 59% at 0.05 and 0.025 mol% of **1**, respectively. The selectivity toward oleyl alcohol was less impacted and remained high (Entries 2 and 3, Table 2). In addition, although the formation of the oleyl oleate is not an issue regarding the tandem reaction (see below), the build-up of this symmetric ester at lower catalyst loading can be explained by its carbonyl function being more difficult to hydrogenate with respect to that of methyl oleate, due to steric effects. Complex **2** bearing more strongly σ–donating isopropyl group at phosphorous atoms proved to be slightly more efficient than **1**, with conversion and selectivity of 73% and 91%, respectively (Entries 2 and 4, Table 2).

As a further step towards implementation of our approach to realistic substrates, we studied the hydrogenation of a commercial FAME mixture, namely RADIA 7060 supplied by Oleon. It consists of a mixture of methyl oleate (monounsaturated C18, 82%), methyl stearate (saturated C18, 7%), methyl palmitate (saturated C16, 4%), and methyl linoleate (2%), to mention the main components only. When performing hydrogenation of RADIA 7060 as received or after deoxygenation by freeze-pump technique, no conversion was observed, which can be ascribed to the presence of impurities acting as poison to the catalyst (Entry 5, Table 2). We assume that trace amounts of peroxides, acids and/or water in the commercial substrate inhibit the formation/regeneration of an active catalytic species. Probably, the presence of acid or/and water induces the formation of carboxylato Ru complexes of general formula $[Ru(H)(CO)(RCOO)(NH\{CH_2CH_2PR'_2\}_2)]$ that is catalytically inactive under base-free conditions, as recently observed for analogous manganese systems in related transformations.[17] This critical issue on impurities within the substrate feed has already been addressed in the case of ruthenium-catalysed olefin metathesis of fatty acid derivatives.[18] The impact of substrate purification on catalytic performances in hydrogenation was thus probed.

Treatment of the substrate with the 3A molecular sieves (MS, 30 wt%), or with activated basic alumina (30 wt%) for 18 h, or by heating at 200 °C for 24 h is not efficient, as no or very little catalytic activity was observed (Entries 6, 7 and 8, Table 2). Interestingly, when the substrate was subjected to consecutive treatment with activated basic alumina (30 wt%) for 18 h, and storage over MS 3A MS (30 wt%) for 48 h, conversion rose to 94%, with an excellent selectivity toward oleyl alcohol of 96% (Entry 9, Table 2). Under similar conditions, complex **2** displayed similar catalytic performances (Entry 10, Table 2). Alternatively, when the substrate was first thermally treated at 200°C under argon stream for 18 h and then stored over activated basic alumina (30% w%) for further 18 h, similar high catalytic activity was achieved by both **1** and **2** (Entries 11 and 12, Table 2). Furthermore, when combining the three consecutive feed treatment steps (heating at 200 °C for 18 h, storage over basic alumina for 18 h and storage over 3A MS for 48 h), conversion and selectivity reached up to 97 and 98%, respectively, with small amount (2 %) of oleyl oleate being detected as the sole side-product (Entry 13, Table 2). At higher catalyst loading (0.2 mol% of **1**), excellent catalytic performances were achieved, with conversion and selectivity values of 99% (Entry 14, Table 2). Thus, neat RADIA 7060 can be efficiently and selectively reduced into the corresponding fatty alcohols mixture, when subjected to the optimized purification protocol.

Alternatively, use of a strong base has frequently been proposed to scavenge water or acid traces in the substrate, as well as for maintaining the catalyst under an active form. This prompted us to probe the influence of such an additive. In presence of **1** and *t*BuOK in 0.1 and 1 mol% respective loading, no catalytic activity was observed (Entry 15, Table 2). Under similar conditions (0.1 mol% **1** and 1.0 mol% NaOEt), thermal treatment of the substrate at 200 °C did not lead to any conversion. Increasing the NaOEt loading to 5 mol% allowed to form oleyl alcohol with 86% of conversion and 83% of selectivity. In addition, significant amount of oleyl oleate (17 %) was also formed, due to the base-promoted transesterification. This shows that the pre-treatment procedure described above holds a significant advantage over use of a base in the catalytic system, as it affords better catalytic performances.

At this stage, having established that borohydride derivatives are efficient ester hydrogenation pre-catalysts in the absence of a base, we carried out some studies to account for the formation of the active species, namely either amido-hydride or amino bishydride species.[15,19] Indeed, Guan reported that some induction period occurs when using PNP borohydride group 8 pre-catalysts for ester hydrogenation, which prompted further investigation.[15] Heating a solution of **2** at 110 °C for 14 h affords a new ruthenium $[Ru(H)(BH_3)(CO)(N\{CH_2CH_2P(iPr)_2\}_2)]$ compound, **3** (with 77 % isolated yield). Kinetic parameters for the dehydrogenation of **2** to **3** were determined by applying a first-order kinetic model (see ESI). From the Eyring equation,

View Article Online
DOI: 10.1039/C7GC02764H

the $\Delta H^{\#}$ activation parameter was estimated to about 15.8 kcal·mol^{-1}. The ^{31}P NMR spectrum features a single resonance at 84.9 ppm which is shifted to lower field with respect to that of **2** (77.8 ppm). On the ^{1}H NMR spectrum, the terminal ruthenium hydride resonates as a triplet centred at -11.34 ppm ($^{2}J_{HP}$ = 19 Hz). A broad lower-field signal centred at -7.0 ppm accounting for one proton is assigned to the bridging hydride Ru-*H*-BH_2.[20] The two BH_2 terminal hydrides were further localized at 1.22 ppm thanks to ^{1}H-^{1}H COSY and ^{1}H-^{11}B{^{1}H} HSQC 2D NMR. These observations show that the exchange rate between terminal and bridging boron-bound hydrides is very slow on the NMR time scale at room temperature, in contrast to that for **2** in which -HBH_3 resonates as a single broad signal.[16] In addition, 2D {^{1}H-^{15}N} HSQC sequence allowed determining the ^{15}N chemical shift of Ru-N-BH_3 to be of 38.0 ppm, indicating sp^3 hybridation.[16] IR spectrum shows an intense band at 1908 cm^{-1} characteristic of terminal CO ligand, and strong signals accounting for B-H-related vibrations in the 2430-2340 cm^{-1} region. The molecular structure of **3** was confirmed by single crystal X-ray diffraction and is similar to the very recently reported analogous [Fe(H)(BH_3)(CO)(N{$CH_2CH_2P(iPr)_2$}$_2$)] complex.[21] It features a distorted octahedral geometry with the amino-phosphine tridentate ligand coordinated in meridional fashion, the terminal carbonyl and amino moiety in mutually *trans* configuration, and the BH_3 moiety bound onto the complex via a B-N bond and a hydride bridging the Ru and B centers in *trans* position to the terminal Ru-H (Figure 3).

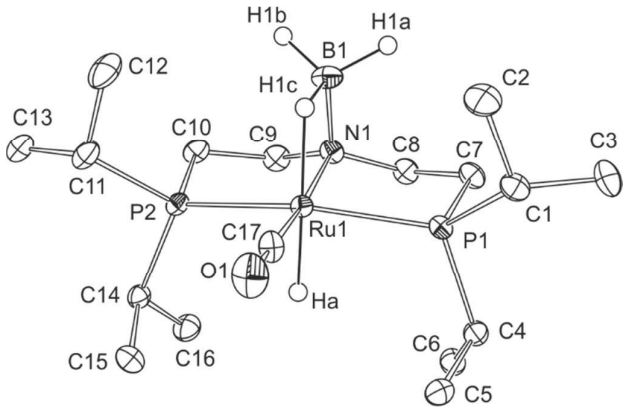

Figure 3. ORTEP view of the solid state structure of **3**. Ellipsoids are given at the 50% probability level. Selected bond lengths (Å) and angles (deg): Ru1-P2 = 2.3082(9), Ru1-P1 = 2.3113(9), Ru1-N1 = 2.133(2), Ru1-C17 = 1.850(3), Ru1-B1 = 2.427(4), Ru1-HA = 1.57(4), Ru1-H1C = 1.64(4), N1-B1 = 1.545(4), B1-H1a = 1.16(3), B1-H1b = 1.10(3), B1-H1c = 1.33(3), P2-Ru1-P1 = 160.72(3), P2-Ru1-B1 = 90.21(12), P2-Ru1-Ha = 80.5(14), P2-Ru1-H1c = 93.6(13), P1-Ru1-B1 = 89.54(12), P1-Ru1-Ha = 86.2(14), P1-Ru1-H1c = 96.2(13), N1-Ru1-P2 = 83.72(8), N1-Ru1-P1 = 84.00(9), N1-Ru1-B1 = 38.95(11), N1-Ru1-Ha = 96.9(13), N1-Ru1-H1c = 70.2(12), C17-Ru1-P2 = 97.12(12), C17-Ru1-P1 = 96.96(12), C17-Ru1-N1 = 172.64(12), C17-Ru1-B1 = 133.69(13), C17-Ru1-Ha = 90.5(13), C17-Ru1-H1c = 102.5(12), B1-Ru1-Ha = 135.8(13), B1-Ru1-H1c = 31.3(12).

In order to get more insights into the generation of catalytic species from **2**, additional experiments were carried out. Heating the solution of pre-catalyst **2** at 105°C for 14 h in the presence of methyl oleate (ca. ~ 10 molar equiv.) and in the absence of hydrogen also generates **3** as a major organometallic species (>80%), along with oleyl alcohol (less than 1 molar equivalent). On the contrary, under similar conditions, heating a solution of **3** in the presence of 10 molar equivalent of methyl oleate did not result in any change. Most likely, the H_2 source for reduction of ester was generated from **2** when converting to **3**. As shown by these NMR studies, both **2** and **3** are thermodynamically more stable than postulated active species **4-H$_2$** and **4** (which are not detected), in line with the very weak Lewis base character of the ester (Scheme 2).[19,22] It can be expected that in the presence of a weak Lewis base such as the ester substrate, the catalytically active amido species **4** (or **4-H$_2$**, Scheme 2) is reversibly formed in solution from **2** or **3**, and thus catalyzes the reduction of the ester in to the alcohol, as reported here.

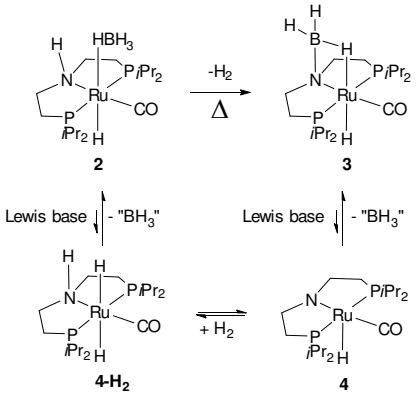

Scheme 2. Proposed pathways to catalytically active **4-H$_2$** and **4** species.

Having optimized the first step of the targeted two-step catalytic sequence, we proceeded to the implementation of the second stage, namely the acceptorless dehydrogenative coupling (ADC) of alcohols into symmetric esters,[23] that we studied in its base-free version as mediated by **1**, **2** and related ruthenium complexes.[16] In the present case, the hydrogenation step affords a stoichiometric mixture of fatty alcohol and methanol. As ADC reaction must proceed under "open" conditions, that is, in a system allowing constant extrusion of hydrogen formed during the alcohol coupling, it can be expected that methanol (with a boiling point of 65°C) will also be stripped off the reaction vessel during the second step, which proceeds at high temperature (typically 130 °C). Thus, the formation of undesired esters resulting from the dehydrogenative hetero-coupling of methanol and fatty alcohols could be strongly inhibited.

We first applied our approach to methyl heptanoate. Using 0.1 mol% **1** loading and after the first hydrogenation step which produced heptanol, the reactor was depressurized, and connected to a nitrogen line, while the temperature was raised up to 130 °C. After 2 h, 99% conversion into heptyl heptanoate as the major product (91% selectivity) was reached, with minor quantity of heptanol (9%) (Entry 1, Table 3). No heptyl formate was detected. The selectivity toward the wax ester is improved up to 99% when the one-pot, two-step synthesis was performed for prolonged reaction times (Entries 2 and 3, Table 3).

View Article Online
DOI: 10.1039/C7GC02764H

Table 2. Base-free hydrogenation of neat methyl oleate and RADIA 7060.[a]

Entry	[Ru] (mol%)	Substrate	Purification and additives	Conversion (%)	Selectivity Alcohol (%)[b]	Selectivity Ester (%)[c]
1	**1** (0.1)	Methyl oleate (99%)	i) 200 °C,18 h ii) Basic alumina,18 h iii) MS 3Å, 48 h.	99	98	2
2	**1** (0.05)			64	95	5
3	**1** (0.025)			59	90	10
4	**2** (0.05)			73	91	9
5	**1** (0.1)	RADIA 7060	-	0	-	-
6	**1** (0.1)		MS 3Å, 48 h	0	-	-
7	**1** (0.1)		200 °C, 18 h	0	-	-
8	**1** (0.1)		Basic alumina, 18 h	7	-	-
9	**1** (0.1)		i) Basic alumina, 18 h ii) MS 3Å, 48 h	94	96	4
10	**2** (0.1)			92	95	5
11	**1** (0.1)		i) 200 °C, 18 h ii) Basic alumina, 18 h	95	96	4
12	**2** (0.1)			94	96	4
13	**1** (0.1)		i) 200 °C,18 h ii) Basic alumina,18 h iii) MS 3Å, 48 h.	97	98	2
14	**1** (0.2)			99	99	1
15	**1** (0.1)		KO*t*Bu, 1.0 mol%	0	-	-
16	**1** (0.1)		i) 200°C, 18 h ii) NaOEt 1.0 mol%	0	-	-
17	**1** (0.1)		i) 200°C, 18 h ii) NaOEt 5.0 mol%	86	83	17

[a]: V(substrate) = 6.12 g (20.63 mmol), 110 °C, 20 bar, 2 h, 1200 rpm; [b]: Selectivity towards formation of alcohol; [c]: Selectivity towards formation of symmetric ester.

Under similar reaction conditions (0.1 mol% **1**, step 1: 20 bar H_2, 110°C, 2 h, step 2: 130 °C, 2 h), 96% of methyl oleate was converted, with oleyl oleate being formed with a selectivity of 92%. Catalyst **2** allows improving the selectivity toward wax ester up to 99% while conversion remains unchanged (Entry 6, Table 3). Lowering the catalyst loading of **1** or **2** at 0.05 mol% is detrimental to both conversion and selectivity (Entries 5 and 7, Table 3). As observed above, these results also confirm the slightly higher catalytic activity of **2** with respect to that of **1**.

Table 3. One-pot, two-step synthesis of wax esters via consecutive Ru-catalysed hydrogenation-dehydrogenation sequence.[a]

Entry	[Ru] (mol %)	Substrate	Step 1			Step 2		Conversion (%)	Selectivity[b] (%)
			T (°C)	t (h)	P(H_2, bar)	T (°C)	t (h)		
1	**1** (0.1)	Methyl heptanoate	110	1	20	130	1	99	91
2	**1** (0.1)		110	1	20	130	2	99	94
3	**1** (0.2)		110	2	20	130	2	99	99
4	**1** (0.1)	Methyl oleate (99%, Sigma Aldrich)	110	2	20	130	2	96	92
5	**1** (0.05)		110	2	20	130	2	66	35
6	**2** (0.1)		110	2	20	130	2	96	99
7	**2** (0.05)		110	2	20	130	2	72	58
8	**1** (0.1)	RADIA 7060	110	2	20	130	2	92	70
9	**1** (0.2)		110	2	20	130	2	96	91
10	**2** (0.1)		110	2	20	130	2	93	98
11	**2** (0.2)		110	2	20	130	2	97	99

[a]: 1200 rpm, n(substrate) = 20.63 mmol, [b]: Selectivity towards wax ester formation after the two steps.

View Article Online
DOI: 10.1039/C7GC02764H

Journal Name

ARTICLE

The reaction sequence was applied to RADIA 7060: In the presence of **1** (0.1 mol%), the conversion rate is 92 %, thus in the same range than with methyl oleate. The selectivity toward wax ester is lower, with only 70% (Entry 8, Table 3). Complex **2** bearing better δ-donor pincer ligand proved more selective, with a higher selectivity toward wax ester of 98% (Entry 10, Table 3). Performing the reaction at higher catalyst loading (0.2 mol%) is beneficial to both conversion rate and selectivity: Under these optimized conditions, the one-pot sequential transformation affords the wax esters mixture with almost full conversion and selectivity (97 and 99%, respectively, entries 9 and 11, Table 3).

In order to probe their potential application, some physicochemical properties of the synthesized wax esters were further determined and compared to those of commercial jojoba oil (Table 4). Indeed, the wax esters found in this oil, which has many benefits in cosmetics for example, have a chemical structure close to that of the esters synthesized in the present work. The density of the considered esters are fully in line with that of the oil. From thermogravimetric analyses (See ESI), the degradation temperature for the fatty wax esters (Entries 1, 2 and 3, Table 4) is comparable, being close to 300 °C. Melting point is also an important feature for oils as it can impact their use and handling. Generally speaking, melting point is directly connected to the chemical structure of the oil, in particular to the number of carbons, substitutions and unsaturations within the alkyl chains (the presence of unsaturations lowers the melting point, see for instance oleyl oleate, T_m= -8 °C, and stearyl stearate, T_m= 62 °C)[24]. The presence and position of an ester function within the alkyl chain also impacts notably the melting point as shown for a series of monoester-based surfactants.[25] It is noteworthy that the melting point of the synthesized esters is lower than that of jojoba oil from about 20 °C and in connection with this property, they are also less viscous. This discrepancy compared to jojoba oil cannot be simply explained as this oil is a complex mixture but it can be pointed out that the values found for the synthesized esters are very suitable for an application in cosmetics. Finally, we have also measured the surface tension of the oils as this property plays an important role in a number of processes where there is a liquid-gas interface; for instance, it drives the wetting of a solid surface by the oil. In cosmetics, the spreadability of oils on the human skin reflects both the sensory qualities and the efficacy of the product and the film forming properties can be partly correlated to the surface tension of the cosmetic oil: the lower the surface tension of the oil, the more spreadable the oil. In the present case, the esters produced from RADIA 7060 feature a surface tension value that is highly similar to that of jojoba oil while that of oleyl oleate is even lower. Thus, these combined elements show that the wax esters prepared from the herein described one-pot procedure from FAMEs affords oils with properties comparable and even better to those of a benchmark product.

Table 4. Physicochemical properties of synthesized esters and jojoba oil.

Entry	Compound	Viscosity[a] (mPa/s)	density[a] (20 °C)	T_{deg}[b] (°C)	T_m[c] (°C)	σ_{surf}[d] (mN/m)
1	Oleyl oleate	29.46	0.8635	300	-8	27.0
2	Esters from RADIA 7060	26.78	0.8689	287	-10	31.9
3	Jojoba oil	45.72	0.8655	289	13	31.7

[a]: Values determined at 20 °C; [b]: T_{deg}: Degradation temperature, determined from TGA initial slope value; [c]: Melting temperature determined from DSC, [d]: Surface tension determined by tensiometry

Conclusions

One-pot, two-step synthesis of wax symmetric esters was successfully conducted by consecutive homogenously ruthenium-catalysed hydrogenation and dehydrogenation reactions of fatty acid methyl esters. This proceeds in the absence of a base additive, and under solvent-free conditions. Using optimized conditions, excellent conversion and selectivity were reached starting from a commercial FAME mixture, affording wax esters that display physicochemical properties up to those of competitive commercial products, such as jojoba oil. This validates the interest of this simple and efficient access to specific cosmetic oils. The present study thus paves the way for further larger implementation of this catalytic approach, which affords wax esters from readily available bioresources, with applicative properties comparable to those of oils extracted from less available natural sources.

Experimental

General considerations. All experiments were carried out under argon atmosphere using a glovebox or a vacuum line using standard Schlenk techniques unless specified. Complexes and ligands were stored under argon. Methyl heptanoate (99%) and methyl oleate (99%) were purchased from Aldrich. RADIA 7060 was supplied by Oleon. MS 3A and alumina were thermally activated at respectively 250 and 300°C for 2h prior use. Methyl heptanoate was distilled under reduced pressure and stored over activated 3A MS (30 wt%) prior use. Both methyl oleate and RADIA were purified according to the following procedure: Under argon stream, the substrate was

View Article Online
DOI: 10.1039/C7GC02764H

heated at 200 °C for 18 h and then outgassed; Next, inside the glove box, the methyl ester was consecutively stored over activated alumina (30 wt%) for 18 h and further passed through a short plug of activated alumina and finally stored over activated 3A MS (30 wt%) for 48 h prior use. Deuterated solvents were purchased from Eurisotop and dried, distilled and outgassed. Ligand [{(*i*Pr)$_2$PCH$_2$CH$_2$}$_2$NH], [RuHCl(CO)(PPh$_3$)$_3$], **1** (trade name: Ru-MACHO-BH) were purchased from Strem Chemicals. Previously reported complex **2** was prepared following literature procedure.[16] All NMR spectra were recorded on Bruker Avance 300/400 NMR spectrometers. ^{1}H and ^{13}C NMR chemical shifts are reported in ppm (δ) downfield from tetramethylsilane, ^{31}P NMR chemical shifts are reported in ppm (δ) and referenced to an external 85 % solution of phosphoric acid in D_2O, ^{15}N NMR chemical shifts are reported in ppm (δ) downfield from an external liquid ammoniac reference. ^{11}B NMR chemical shifts are reported in ppm (δ) and referenced to external solution of $BF_3.Et_2O$. Common abbreviations used in the NMR experiments are as follows: b, broad; s, singlet; d, doublet; t, triplet; q, quartet; sp, septet; m, multiplet; v, virtual. Spectral assignments were made by means of routine one- (^{1}H, ^{1}H{^{31}P), ^{31}P{^{1}H}, ^{13}C{^{1}H}, ^{13}C JMOD, ^{11}B, ^{11}B{^{1}H}) and two-dimensional (^{1}H-^{1}H COSY, ^{1}H-^{1}H NOESY, ^{1}H-^{13}C HSQC, ^{1}H-^{13}C HMBC, ^{1}H-^{15}N HSQC, ^{1}H-^{15}N HMBC…) NMR experiments where appropriate. IR spectra were recorded on a Nicolet 6700 FT-IR spectrometer equipped with a Praying Mantis mirror chamber (from Harrick Scientific) by using a DRIFT cell equipped with KBr windows. The samples were prepared under argon in a glove-box. Typically, 64 scans were accumulated for each spectrum (resolution 4 cm^{-1}). Data are reported as follows: weak (w), medium (m), strong (s) and very strong (vs).

Synthesis of [Ru(H)(BH$_3$)(CO)({(*i*Pr)$_2$PC$_2$H$_4$}$_2$N)] (**3**). The solution of [Ru(H)(BH$_4$)(CO)({(*i*Pr$_2$)PC$_2$H$_4$}$_2$NH)] (**2**, 0.44 mmol, 0.2 g) in toluene (15 mL) was heated at 110°C for 14h. The resulting solution was evaporated to dryness under reduced pressure and extracted with *n*-pentane. Extracts were filtered and concentrated under reduced pressure. Colorless crystals were obtained upon storage of the solution at -18°C (0.153 g, 77 % yield). A single crystal suitable for X-ray determination was obtained by a similar method. FT-IR (KBr, cm^{-1}): ν(BH) = 2430 (s), 2396 (s), 2360 (m), 2340 (s), *ν*(CO) = 1908 (s). ^{1}H NMR (300 K, C_6D_6, 400.13 MHz, ppm): *δ* 3.02 (m, 2H, >CH$_2$, J_{HH} = 7.8 Hz), 2.18 (m, 2H, >CH$_2$), 2.02 (m, 2H, >CH$_2$, J_{HH} = 7.3, 14.0 Hz, J_{HP} = 2.8 Hz), 1.86 (m, 2H, >CH-, J_{HH} = 7.3 Hz), 1.70 (m, 2H, >CH-, J_{HH} = 7.1 Hz), 1.45 (2H, N-BH$_2$), 1.22 (m, 2H, >CH$_2$, J_{HH} = 5.4, 14.0 Hz), 1.18 (dt, 6H, -CH$_3$, J_{HH} = 7.2 Hz, J_{HP} = 7.1 Hz), 1.12 (dt, 6H, -CH$_3$, J_{HH} = 6.3 Hz, J_{HP} = 7.5 Hz), 1.10 (dt, 6H, -CH$_3$, J_{HH} = 6.9 Hz, J_{HP} = 7.0 Hz), 1.0 (dt, 6H, -CH$_3$, J_{HH} = 6.9 Hz, J_{HP} = 6.9 Hz), -7.0 (b, 1H, B-H-Ru), -11.33 (t, 1H, RuH, J_{HP} = 19.2 Hz). ^{31}P{^{1}H} NMR (300 K, C_6D_6, 162.057 MHz, ppm): *δ* 84.9 (s, 2P). ^{13}C{^{1}H} NMR (300 K, C_6D_6, 100.663 MHz, ppm): *δ* 206.77 (t, 1C, CO, J_{CP} = 11.2 Hz), 59.90 (t, 2C, >CH$_2$, J_{CP} = 3.7 Hz), 27.62 (t, 2C, >CH-, J_{CP} = 11.1 Hz), 25.67 (t, 2C, >CH-, J_{CP} = 13.8 Hz), 24.55 (t, 2C, >CH$_2$, J_{CP} = 8.7 Hz), 19.38 (2C, -CH$_3$), 19.32 (2C, -CH$_3$), 18.93 (2C, -CH$_3$), 18.59 (2C, -CH$_3$). ^{11}B{^{1}H} NMR (300 K, C_6D_6, 128.442 MHz, ppm): *δ* -25.64 (s, 1B). ^{15}N{^{1}H} HMBC NMR (300 K, C_6D_6, 40.565 MHz, ppm): *δ* 38.6 (1N). ^{1}H-^{1}H COSY (225 K, C_7D_8, 400.33 MHz, ppm, selected data): *δ* 1.45 (2H, N-BH$_2$). Anal. Calcd. For $C_{17}H_{40}BRuNOP_2$: C 45.54; H 8.99; N 3.12. Found: C 45.44; H 8.94; N 3.05.

Kinetic studies. The kinetic parameters for the dehydrogenation of **2** to **3** were determined by NMR spectroscopy. First-order rate constants were determined from the decay of [**2**] with time under first-order conditions using linear least-square regression analysis. Typical plots of [**2**] and [**3**] obtained from NMR measurements using 10 mg of **2** in 0.45 mL of toluene-d8 ([**2**]$_0$ = 0.0493 mmol.mL^{-1}) are given in ESI. The ln([**2**]) vs. time representation provided a linear fit that is representative of a first-order kinetic transformation with the slope of the line corresponding to the observed first-order rate constant k_{obs} (see ESI).

X-ray Structure Determination. A single crystal of **3** was mounted under inert perfluoropolyether wax on a Mitegen MicroLoopTM. The single-crystal X-rays measurements were performed at 100 K under N_2 stream from a Cryostream 700 device (OxfordCryosystems). Data were collected using an Apex II CCD 4K Bruker diffractometer (λ = 0.71073 Å). The structures were solved using SHELXT and refined by least-squares procedures on F2 using SHELXL2014.[26,27] All the hydrogen atoms were placed in theoretical positions and refined riding on their parent atoms except for the hydride H attached to the Ru atom and the H atoms bound to the B atom, which were located from difference Fourier maps and refined isotropically. ORTEP drawings were generated with ORTEP-3.[28] Crystallographic data have been deposited at the Cambridge Crystallographic Data Centre as Supplementary Publication Nos. CCDC 1557611. Copies of the data can be obtained free of charge on application to the Director, CCDC, 12 Union Road, Cambridge CB2 1EZ, U.K. (fax, (+44) 1223- 336-033; e-mail, deposit@ccdc.cam.ac.uk).

Catalytic experiments. Under nitrogen stream, catalyst (**1** or **2**) was added to a 110 mL autoclave equipped with a mechanical stirring system. The reactor was sealed and placed under vacuum and flushed with nitrogen. Next, substrate (20.63 mmol) was added under nitrogen stream. The reactor was further purged with H_2 (10 bar) several times and pressurized to the desired pressure (10 or 20 bar). The reaction mixture was then warmed to reaction temperature and timing started when the desired temperature was reached (90 or 110°C). The experiment was performed under a continuous feed of H_2 gas. For the dehydrogenation step, the reactor was connected to the gas outlet equipped with a bubbling system. The reactor was then slowly depressurized and placed under nitrogen flushing. The reaction medium was further heated at 130°C while stirring. At the end of the reaction, the reactor was cooled to room temperature and the resulting mixture was analyzed by ^{1}H NMR.

Physicochemical property measurements. The surface tensions were determined using a Krüss-K100 tensiometer equipped with plate geometry. They were carried out at 25 °C. The temperature was thermo-regulated thanks to a double-jacketed glass cell by means of a water bath using a Lauda RC6 circulator to control the temperature. Surface tension values

View Article Online
DOI: 10.1039/C7GC02764H

were sampled every three seconds until the standard deviation was below 0.1 mN.m^{-1}. Three measurements were taken for each sample. Thermogravimetric analysis (TGA) of the oils was performed using a TGA Q5000 apparatus (TA Instruments) unit under a nitrogen atmosphere to determine the degradation temperatures. Samples between 2 and 10 mg were placed in aluminum pans and heated from 25 to 400 °C at a heating rate of 10 °C min^{-1}. The degradation temperature T_{deg} was determined as the starting point of the degradation (range with the highest slope of TGA curves). Thermal transitions were determined by differential scanning calorimetry (DSC) with a DSC Q100 calorimeter (TA Instruments) unit under a nitrogen atmosphere, calibrated with a standard sample of indium. Samples between 5 and 10 mg were sealed in aluminum pans and measured over a temperature range of -80 °C until ca. 300 °C under the beginning of degradation with a rate of 10 °C·min^{-1}; the samples were cooled with an intercooler. The phase transitions of the products were investigated, providing the melting temperature (T_m, as onset of an endothermic peak on heating). Viscosities and densities were measured simultaneously using a DMA4100/Lovis2000 densimeter/viscometer from Anton Paar, by rolling a ball through a liquid-filled glass capillary (Ø 1.59 mm) inclined at a defined angle. The liquid's viscosity is directly proportional to the rolling time.

Acknowledgements

This work was performed in partnership with the SAS PIVERT, within the frame of Institut pour la Transition Energétique P.I.V.E.R.T. (www.institut-pivert.com) selected as an Investment for the Future ("Investissements d'Avenir"). This work was supported, as part of the Investments for the Future, by the French Government under the reference ANR-001-01. Chevreul Institute (FR 2638), Ministère de l'Enseignement Supérieur et de la Recherche, Région Nord – Pas de Calais and FEDER are acknowledged for supporting and funding partially this work. We acknowledge Mike Ortega for his help with physicochemical studies, Celine Delabre for GC-MS analysis and Xavier Trivelli (UGSF) for his assistance with NMR measurements.

Notes and references

1 Lipids and Skin Health, A. Pappas, (Ed.), Springer 2015, Chapter 11: Wax Esters: Chapter Chemistry and Biosynthesis, P. E. Kolattukudy, 159-183.
2 Bagby, M.O., Comparison of Properties and Function of Jojoba Oil and Its Substitutes, Proceedings from the Seventh International Conference on Jojoba and Its Uses, American Oil Chemists' Society, Champaign, IL, 1988, 6132.
3 T. K. Miwa, *J. Am. Oil Chem. Soc.,* 1984, **61**, 407-409.
4 O. Thum, *Tenside Surf. Deterg*., 2004, **41**, 287-290.
5 L. Hilterhaus, O. Thum, A. Liese, *Org. Process. Res. Dev*., 2008, **12**, 618-625.
6 M. R. Meneghetti, S. M. Plentz Meneghetti, *Catal. Sci. Technol.,* 2015, **5**, 765-771.
7 J. R. Khusnutdinova, D. Milstein, *Angew. Chem. Int. Ed*., 2015, **54**, 12236-12273.
8 a) S. Werkmeister, J. Neumann, K. Junge, M. Beller, *Chem. Eur. J.,* 2015, **21**, 12226-12250. b) C. Gunanathan, D. Milstein, *Chem. Rev*., 2014, **114**, 12024-12087.
9 a) J. Zhang, G. Leitus, Y. Ben-David, D. Milstein, *Angew. Chem. Int. Ed*., 2006, **45**, 1113-1115. b) E. Fogler, E.Balaraman, Y. Ben-David, G. Leitus, L. J.W. Shimon, D. Milstein, *Organometallics* 2011, **30**, 3826-3833. c) J. Zhang, E. Balaraman, G. Leitus,D. Milstein, *Organometallics* 2011, **30**, 5716-5724. d) Y. Sun, C. Koehler, R. Tan, V. T. Annibale, D. Song, *Chem. Commun*. 2011, **47**, 8349-8351. e) D. Spasyuk, D. G. Gusev, *Organometallics* 2012, **31**, 5239–5242. f) D. Spasyuk, S. Smith, D. G. Gusev *Angew. Chem. Int. Ed*., 2012, **51**, 2772 –2775. g) D. Spasyuk, S. Smith, D. G. Gusev *Angew. Chem. Int. Ed.*, 2013, **52**, 2538 –2542. h) A. Acosta-Ramirez, M. Bertoli, i) D. Spasyuk, C. Vicent, D. G. Gusev, *J. Am. Chem. Soc*., **2015**, 137, 3743–3746. j) G. A. Filonenko, M. J. B. Aguila, E. N. Schulpen, R. van Putten, J. Wiecko, C. Müller, L. Lefort, E. J. M. Hensen, E. A. Pidko, *J. Am. Chem. Soc.*, 2015, **137**, 7620–7623. k) X. Tan, Y. Wang, Y. Liu, F. Wang, L. Shi, K-H. Lee, Z. Lin, H. Lv, X. Zhang, *Org. Lett.,* 2015, **17**, 454-457. l) Tan, Q. Wang, Y. Liu, F. Wang, H. Lv, X. Zhang, *Chem. Commun*., 2015, **51**, 12193-12196. m) O. Ogata, Y. Nakayama, H. Nara, M. Fujiwhara, Y. Kayaki. *Org. Lett*., 2016, **18**, 3894–3897. n) D. Kim, L. Le, M. J. Drance, K. H. Jensen, K. Bogdanovski, T. N. Cervarich, M. G. Barnard, N. J. Pudalov, S. M. M. Knapp, A. R. Chianese, *Organometallics*, 2016, **35**, 982-989. o) Wang, X. Chen, B. Liu, Q-B. Liu, G. A. Solan, X. Yang, W-H. Sun, *Catal. Sci. Technol*., 2017, **7**, 1297-1304.
10 D. G. Gusev, M. Schlaf, *Green Chem*., 2012, **14**, 1178–1188.
11 a) K. Junge, B. Wendt, H. Jiao, M. Beller, *ChemCatChem* 2014, **6**, 2810-2814. b) T. P. Brewster, N. M. Rezayee, Z. Culakova, M. S. Sanford, K. I. Goldberg, *ACS Catal*. 2016, **6**, 3113−3117.
12 a) T. Zell, Y. Ben-David, *D.Milstein, Angew. Chem. Int. Ed.*, 2014, **53**, 4685-4689. b) S. Werkmeister, K. Junge, B. Wendt, E. Alberico, H. Jiao, W. Baumann, H. Junge, F. Gallou, M. Beller, *Angew. Chem. Int. Ed*., 2014, **53**, 8722 –8726. c) S. Chakraborty, H. Dai, P. Bhattacharya, N. T. Fairweather, M. S. Gibson, J. A. Krause, H. Guan, *J. Am. Chem. Soc*., 2014, **136**, 7869−7872.
13 a) G. Zhang, K. V. Vasudevan, B. L. Scott, S. K. Hanson, *J. Am. Chem. Soc.,* 2013, **135**, 8668−8681. b) D. Srimani, A. Mukherjee, A. F. G. Goldberg, G. Leitus, Y. Diskin-Posner, L. J. W. Shimon, Y. Ben David, D. Milstein, *Angew. Chem. Int. Ed.*, 2015, **54**, 12357-12360. c) T. J. Korstanje, J. I. van der Vlugt, C. J. Elsevier, B. de Bruin, *Science*, 2015, **350**, 298-302.
14 a) S. Elangovan, M. Garbe, H. Jiao, A. Spannenberg, K. Junge, M. Beller, *Angew. Chem. Int. Ed.,* 2016, **55**, 15364-15368. b) R. van Putten, E. A. Uslamin, M. Garbe, C. Liu, A. Gonzalez-de-Castro, M. Lutz, K. Junge, E. J. M. Hensen, M. Beller, L. Lefort, E. A. Pidko, *Angew. Chem. Int. Ed*., 2017, **56**, 7531-7534. c) N. A. Espinosa-Jalapa, A. Nerush, L. J. W. Shimon, G. Leitus, L. Avram, Y. Ben-David, D. Milstein, *Chem. Eur. J.,* 2017, **23**, 5934-5938.
15 N. T. Fairweather, M. S. Gibson, H. Guan, *Organometallics* 2015, **34**, 335−339.
16 L. Zhang, G. Raffa, D. H. Nguyen, Y. Swesi, L. Corbel-Demailly, F. Capet, X. Trivelli, S. Desset, P. Paul, J-F. Paul, P. Fongarland, F. Dumeignil, R. Gauvin, *J. Catal*., 2016, **340**, 331-343.
17 a) D. H. Nguyen, X. Trivelli, F. Capet, J-F. Paul, F. Dumeignil, R. M. Gauvin, *ACS Catal*., 2017, **7**, 2022–2032. b) D. H. Nguyen, Y. Morin, L. Zhang, X. Trivelli, F. Capet, S. Paul, S. Desset, F. Dumeignil, R. M. Gauvin, *ChemCatChem*. 2017, **9**, 2652-2660 ; D. H. Nguyen, R. M. Gauvin, unpublished results.
18 a) J. Bidange, J.-L. Dubois, J.-L. Couturier, C. Fischmeister, C. Bruneau, *Eur. J. Lipid Sci. Tech*., 2014, **116**, 1583-1589; b) P. Vignon, T. Vancompernolle, J.-L. Couturier, J.-L. Dubois, A.

View Article Online
DOI: 10.1039/C7GC02764H

Mortreux, R. M. Gauvin, *ChemSusChem*, 2015, **8**, 1143-1146. c) J. Allard, I. Curbet, G. Chollet, F. Tripoteau, S. Sambou, F. Caijo, Y. Raoul, C. Crévisy, O. Baslé, M. Mauduit, *Chem. Eur. J.*, 2017, DOI: 10.1002/chem.201703049.
19 S. Qu, H. Dai, Y. Dang, C. Song, Z-X. Wang, H. Guan, *ACS Catal*., 2014, **4**, 4377−4388.
20 Y. Xu, C. A. Rettenmeier, G. T. Plundrich, H. Wadepohl, M. Enders, L. H. Gade, *Organometallics*, 2015, **34**, 5113−5118.
21 F. Anke, D. Han, M. Klahn, A. Spannenberg, T. Beweries *Dalton Trans*., 2017, **46**, 6843–6847.
22 C. A. Sandoval, T. Ohkuma, K. Muniz, R. Noyori, *J. Am. Chem. Soc.,* 2003, **125**, 13490-13503.
23 a) J. Zhang, G. Leitus, Y. Ben-David, D. Milstein, *J. Am. Chem. Soc*., 2005, **127**, 10840-10841. b) D. Kim, L. Le, M. J. Drance, K. H. Jensen, K. Bogdanovski, T. N. Cervarich, M. G. Barnard, N. J. Pudalov, S. M. M. Knapp, A. R. Chianese, *Organometallics*, 2016, **35**, 982−989. c) E. Fogler, J. A. Garg, P. Hu, G. Leitus, L. J. W. Shimon, D. Milstein, *Chem. Eur. J*., 2014, **20**, 15727-15731. d) K-N. Tseng, J. W. Kampf, N. K. Szymczak, *Organometallics,* 2013, **32**, 2046−2049. e) S. Musa, S. Fronton, L. Vaccaro, D. Gelman, *Organometallics*, 2013, **32**, 3069−3073. f) C. Chen, Y. Zhang, S. H. Hong, *J. Org. Chem*. 2011, 76, 10005−10010. g) C. del Pozo, M. Iglesias, F. Sanchez, *Organometallics,* 2011, **30**, 2180–2188. h) M. Bertoli, A. Choualeb, A. J. Lough, B. Moore, D. Spasyuk, D. G. Gusev, *Organometallics,* 2011, **30**, 3479–3482. i) M. Nielsen, A. Kammer, D. Cozzula, H. Junge, S. Gladiali, M. Beller, *Angew. Chem. Int. Ed*., 2011, **50**, 9593-9597.
24 B. T. R. Iyengar, H. Schlenk, *Lipids*, 1968, *4*, 28-30.
25 V. Nardello, N. Chailloux, G. Joly and J-M. Aubry, *Coll. Surf. A.: Physicochem. Eng. Aspects*, 2006, **288**, 86-95.
26 G. M. Sheldrick, *Acta Cryst*., 2015, **A71**, 3-8.
27 G. M. Sheldrick, *Acta Cryst*., 2015, **C71**, 3-8.
28 L. J. Farrugia, *J. Appl. Crystallogr*., 1997, **30**, 565.

View Article Online
DOI: 10.1039/C7GC02764H

Wax esters were produced from fatty acid methyl esters using a catalytic one-pot, two-step sequence under solvent- and base-free conditions.